A LETTERS JOURNAL EXPLORING THE FRONTIERS OF PHYSICS

January 2009

EPL, **85** (2009) 14003 www.epljournal.org
doi: 10.1209/0295-5075/85/14003

Enhanced wave absorption through irregular interfaces

S. Félix[1], B. Sapoval[1,2], M. Filoche[1,2(a)] and M. Asch[3]

[1] *Physique de la Matière Condensée, Ecole Polytechnique, CNRS - 91128 Palaiseau, France, EU*
[2] *CMLA, ENS Cachan, CNRS, UniverSud - 61 Avenue du President Wilson, F-94230 Cachan, France, EU*
[3] *LAMFA, Université de Picardie Jules Vernes CNRS - 80039 Amiens, France, EU*

received 16 September 2008; accepted in final form 26 November 2008
published online 13 January 2009

PACS 42.60.Da – Resonators, cavities, amplifiers, arrays, and rings
PACS 43.55.+p – Architectural acoustics
PACS 73.20.Fz – Weak or Anderson localization

Abstract – The diffraction and absorption of waves by a system with both absorbing properties and irregular geometry is an open physical problem. A more reachable and closely related question is the understanding of wave oscillations in confined systems containing an absorbing material with an irregular shape. This has to be solved to understand why anechoic chambers (electromagnetic or acoustic) do work better with irregular absorbing walls. The answer to this question could also be used in other fields such as light or microwave absorption, or also to improve the performances of break-waters in order to damp sea-waves. It is found here that, in resonators containing an irregular shaped absorbent material, there appears a new type of mode localization. This phenomemon, that we call "astride" localization, describes the fact that these modes exist in both the lossless and the lossy regions. It is these modes that are particularly efficient in dissipating the energy of waves excited in the non-absorbing region.

Simple to study in classical geometries, closed resonators exhibit nontrivial localization effects as soon as the confining geometry exhibits some kind of irregular behavior [1–7]. If the surface of the resonator is itself absorbing, these localization effects give rise to a specific enhancement of the damping [8]. Concerning dissipation in the bulk however, the only mathematical result concerning this problem has been given in 2D for geometries that are smooth at the scale of the wavelength [9]. In that situation, it was shown that the modes are localized either in the non-absorbing region, with approximately real eigenvalues, or are localized in the absorbing region, with eigenvalues having a large imaginary part. The qualitative consequence is that waves excited in the non-absorbing region stay mostly in the same region and are thus poorly dissipative. Conversely, strongly dissipative modes localized in the dissipative regions are poorly coupled to sources in the non-absorbing regions due to their small amplitude in these regions. So, strongly dissipative modes are poorly coupled and strongly coupled modes are poorly dissipative: in both cases the system is poorly absorbing due to localization.

In this work, we show, on two examples, that if one wishes to absorb waves, the above dilemma can be lifted by using an irregular geometry for the interface between the absorbing and the non-absorbing medium. We consider two situations: an electromagnetic and an acoustic shallow cavity Ω, in which the fields obey simple scalar wave equations. The cavity is rectangular (fig. 1) but its global shape has no significant effect on the qualitative results that are described below. In a region $\Omega_0 \subset \Omega$, the cavity is filled with a homogeneous and lossless medium, while on the complementary part $\Omega_\mathrm{d} = \Omega - \Omega_0$, the homogeneous medium is dissipative and possibly dispersive. Let us call Γ the interface, of arbitrary shape, between the two media. Thus, the eigenvalue problem can be written

$$\begin{cases} \Delta\psi_i = -k_i^2\psi_i & \text{in } \Omega_0, \\ \Delta\psi_i = -k_i^2 n^2(\omega)\psi_i & \text{in } \Omega_\mathrm{d}, \end{cases} \tag{1}$$

with the classical continuity conditions on Γ. The quantity $n(\omega) \in \mathbb{C}$ is the complex refraction index of the dissipative medium.

For a shallow horizontal electromagnetic cavity, the field ψ_i is the vertical electric field obeying the Dirichlet condition $\psi_i = 0$ on the outer metallic boundary. For a shallow acoustic cavity, the field ψ_i is the acoustic pressure

(a) E-mail: marcel.filoche@polytechnique.edu

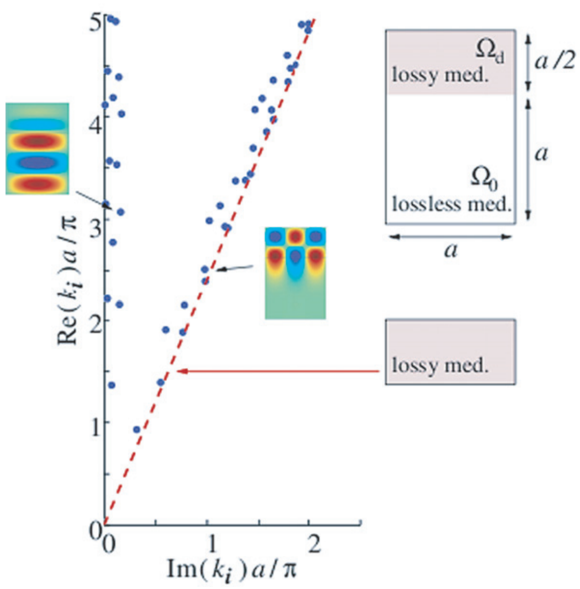

Fig. 1: (Colour on-line) Low-frequency complex eigenvalues for the electromagnetic cavity with a planar absorbent material as shown on the top right. Relative dielectric constant and permittivity are both equal to 1 in the lossless medium, and equal to $2-2\mathrm{j}$ and 1, respectively in the lossy medium. The dashed red line shows the location of the theoretical eigenvalues of a single cavity filled with the same lossy medium.

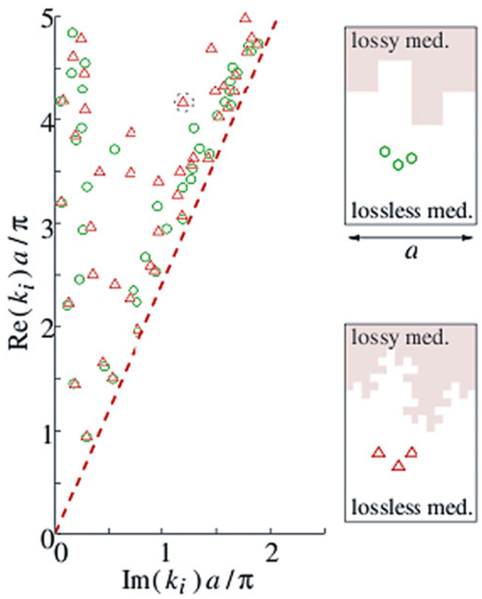

Fig. 2: (Colour on-line) Low-frequency complex eigenvalues for the two electromagnetic cavities with irregular absorbers as shown on the right. Green circles (respectively, red triangles) correspond the first (respectively, second) generation of the prefractal interface. Dielectric constants and permittivities are the same as in fig. 1. The dashed red line shows the location of the theoretical eigenvalues of a single cavity filled with the lossy medium. The dotted circle corresponds to the eigenvalue of the mode displayed in fig. 4(a).

field obeying the Neumann condition on the boundary: $\vec{\nu}\cdot\vec{\nabla}\psi_i=0$, with $\vec{\nu}$ the normal to the surface.

In the first example under consideration —an electromagnetic cavity with Dirichlet boundary conditions— the lossless medium is characterized by a relative permitivity ϵ_0 and permeability μ_0 both equal to 1, while the corresponding values in the lossy medium are chosen arbitrarily as $\epsilon_\mathrm{d}=2-2\mathrm{j}$ and $\mu_\mathrm{d}=1$. Although both quantities should really depend on the frequency, no specific frequency dependance is needed to observe the localization effect we are interested in.

The numerical results discussed below have been obtained using a P2 finite element scheme and solving libraries from FEMLAB®. When the interface between the two media in the cavity is planar, the spectrum of eigenvalues k_i is distributed in the complex plane as shown in fig. 1. In this figure, one clearly distinguish two families of eigenmodes, each following approximately a simple theoretical limit. The first family have nearly real eigenvalues, and their amplitude distributions show that the corresponding modes are mostly localized in the lossless region of the cavity, with a rapid decrease in the lossy region. The second family is composed of eigenmodes localized in the lossy region of the cavity, and the corresponding eigenvalues are concentrated along the dashed line. This line is the support of the theoretical eigenvalues of an isolated cavity Ω_d filled with the lossy medium. This case can be easily calculated. Indeed, consider a shallow cavity $\mathcal{C}$ of arbitrary shape, filled with a medium having a refraction index $n(\omega)\in\mathbb{C}$, with homogeneous Dirichlet or Neumann condition on the boundary. Solving the eigenvalue equation $\Delta\psi_i=-k_i^2n^2(\omega)\psi_i$ in $\mathcal{C}$ leads to a set of discrete *real* values $\delta_i=k_in$. Writing that δ_i is real implies that, in the complex plane $(\mathrm{Im}(k),\mathrm{Re}(k))$ the eigenvalues k_i are located on the curve $(-\mathrm{Re}(k)\mathrm{Im}(n)/\mathrm{Re}(n),\mathrm{Re}(k))$. In the present case where the refraction index $n=\sqrt{2-2\mathrm{j}}$ is chosen to be frequency independent, this curve is the dashed line shown in fig. 1. Thus, the inhomogeneous resonator Ω, with a planar separation between the two subdomains, behaves essentially as two *decoupled* resonators Ω_0 and Ω_d.

We now consider the role played by the irregular character of the geometry of the interface between the two media. By this, we mean that the interface exhibits geometrical irregularities whose sizes are of the order of the wavelengths under consideration. We use first and second generations of the quadratic Koch curve (fractal dimension equal to 3/2) in order to increase the irregularity while keeping constant the quantity of dissipative material (fig. 2). Now, the well discriminated undamped and damped eigenmodes found for the planar interface are replaced by an ensemble of modes with eigenvalues widely spread in the complex plane. The eigenvalues occupy a region delimited by the two theoretical limits described above. There are still a few values close to the former theoretical limits, but most of the modes now are found

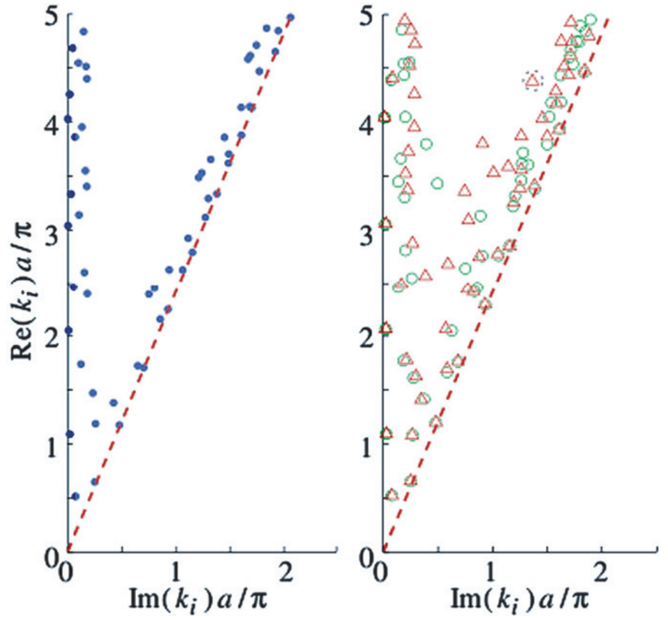

Fig. 3: (Colour on-line) Low-frequency complex eigenvalues of acoustic cavities as shown on the right of figs. 1 and 2. Blue dots (respectively, green circles and red triangles) correspond the zeroth (respectively, first and second) generation of the prefractal interface. Relative density and compressibility are both equal to 1 in the lossless medium, and 1 and $(2-2\mathrm{j})^{-1}$ in the lossy medium. The dashed red line shows the location of the theoretical eigenvalues of a single cavity filled with the same lossy medium as described above. The dotted circle on the right plot corresponds to the eigenvalue of the mode displayed in fig. 4(b).

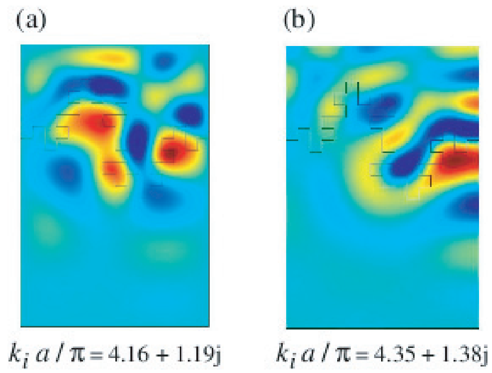

Fig. 4: (Colour on-line) Examples of astride localization of modes located at the irregular interface in (a) an electromagnetic cavity (Dirichlet boundary condition), (b) an acoustic cavity (Neumann boundary condition). The "astride" characters of these modes (see below) are, respectively, $\eta = 0.2412$ and $\eta = 0.2489$.

between these limits, and the number of these modes increases with the irregularity of the interface.

This type of behavior is general and can be observed in analogous wave systems. For example, a shallow acoustic cavity, now obeying Neumann boundary conditions,

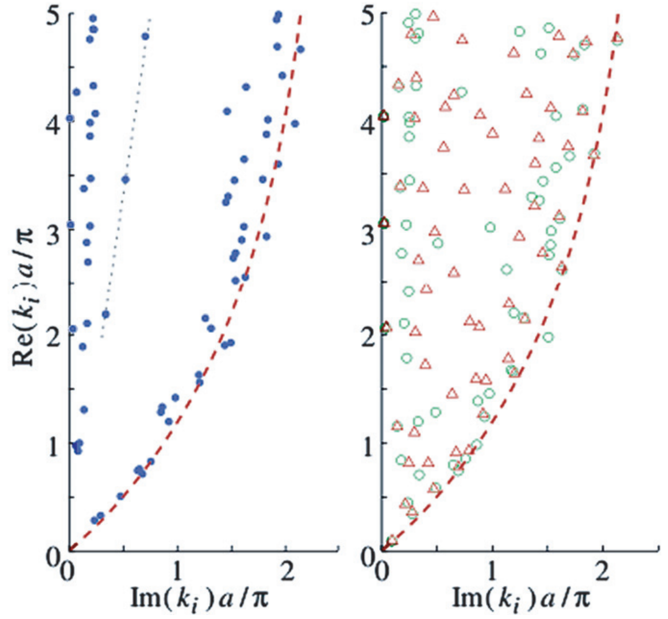

Fig. 5: (Colour on-line) Eigenvalues in the same geometries for dispersive and a realistic absorbing acoustic material. Blue dots (respectively, green circles and red triangles) correspond the zeroth (respectively, first and second) generation of the prefractal interface. Relative density and compressibility are 1 and 1 in the lossless medium, while in the lossy medium they are those of a porous medium in the equivalent fluid assumption. The material used here is a typical polyurethane foam at audio frequencies [10]. The dashed curve shows the location of the theoretical eigenvalues of a single cavity filled with the same medium. The dotted line on the left plot shows some of the classical "interface" modes that may arise on a plane interface.

exhibits the same kind of results as shown in fig. 3. Here the lossless medium is characterized by a relative density ρ_0 and a relative compressibility K_0 both equal to 1 [10], while the corresponding values in the lossy medium are $\rho_{\mathrm{d}} = 1$ and $K = (2-2\mathrm{j})^{-1}$, so that $n = \sqrt{2-2\mathrm{j}}$ as in the electromagnetic case above.

A major characteristic is that the amplitude distribution of the modes corresponding to these *intermediate* eigenvalues are located *around* the irregular interface. Examples for both the electromagnetic and acoustic cases are shown in fig. 4. These are what we call "astride" modes and the number of these astride modes increases with increasing irregularity.

The existence of frequency dispersion in the absorbent properties of course modify the details of the spectrum but astride modes remains present. For example, one now considers a medium whose dispersion relation is typical of a porous acoustic material, modelled as an equivalent fluid [10]. The eigenvalues spectra are shown in fig. 5. Note that, due to the dependence of the refraction index n on the frequency, the theoretical limit case for the lossy modes (red dashed line) is no longer a straight line, but a curve.

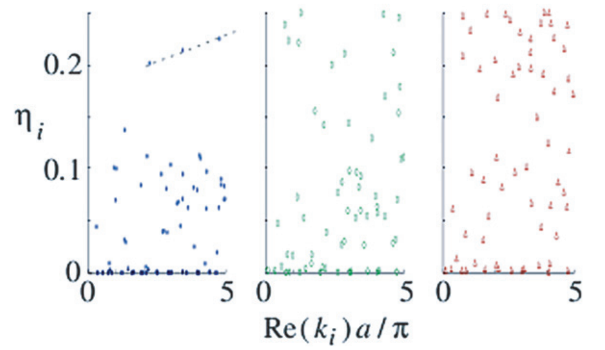

Fig. 6: (Colour on-line) Values of the astride character $\eta_i = S_i^{(\Omega_0)} S_i^{(\Omega_\mathrm{d})}/S_i^2$ for the eigenmodes of the acoustic cavities already considered in fig. 5. Blue dots (respectively, green circles and red triangles) correspond the zeroth (respectively, first and second) generation of the prefractal interface. In the flat case, the dotted line indicates three classical "interface" modes (see fig. 5).

To characterize more precisely the astride modes, it is useful to introduce a measure of the confinement of the spatial amplitude distribution of the modes. The confinement of a mode ψ_i, normalized by $\int_\Omega |\psi_i|^2\,\mathrm{d}S = 1$, is classically characterized by its "existence" surface [11,12]

$$S_i = \frac{1}{\int_\Omega |\psi_i|^4\,\mathrm{d}S}. \tag{2}$$

But rather than the existence surface itself, it is more interesting here to consider how the amplitude distribution of the eigenmodes is distributed over both the lossless and the lossy regions. This can be done by writing the existence surface S_i as a sum of two existence surfaces, respectively in the lossless and in the lossy region:

$$S_i^{(\Omega_0)} = S_i \times \left(\frac{\int_{\Omega_0} |\psi_i|^4\,\mathrm{d}S}{\int_\Omega |\psi_i|^4\,\mathrm{d}S} \right) = S_i^2 \int_{\Omega_0} |\psi_i|^4\,\mathrm{d}S, \tag{3}$$

$$S_i^{(\Omega_\mathrm{d})} = S_i \times \left(\frac{\int_{\Omega_d} |\psi_i|^4\,\mathrm{d}S}{\int_\Omega |\psi_i|^4\,\mathrm{d}S} \right) = S_i^2 \int_{\Omega_\mathrm{d}} |\psi_i|^4\,\mathrm{d}S. \tag{4}$$

These quantities obey the natural additivity rule $S_i = S_i^{(\Omega_0)} + S_i^{(\Omega_\mathrm{d})}$. One can then compute the product $\eta_i = S_i^{(\Omega_0)} S_i^{(\Omega_\mathrm{d})}/S_i^2$. This quantity would be equal to 0 both for modes localized only in the lossless or the lossy regions. It can then be considered as a simple measure of the "astride" character of a mode.

Figure 6 gives the values of η_i for the eigenmodes of the three acoustic cavities considered above, that is, with the generations 0, 1, and 2 of the Koch curve as the interface between the two media. One clearly observes a net increase of the number of astride modes with increasing irregularity. The average values $\langle \eta_i \rangle$ are, respectively, 0.05, 0.08, and 0.12 for the generations 0, 1, and 2 of prefractal geometry.

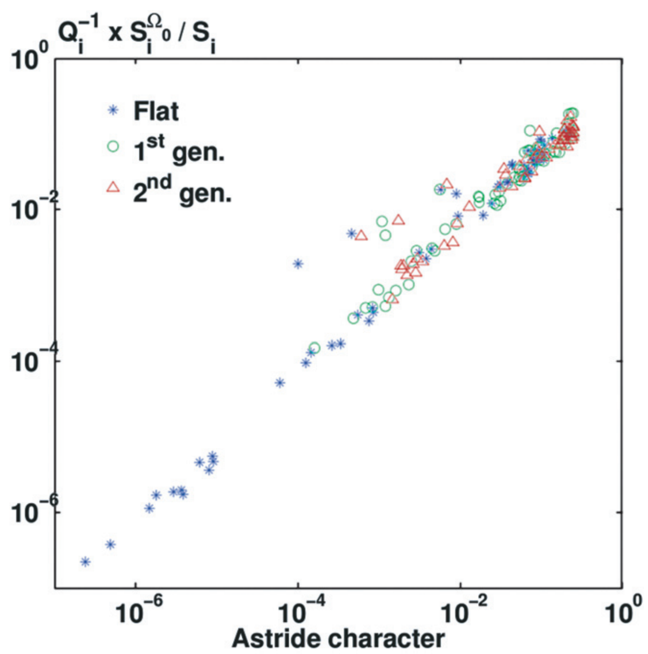

Fig. 7: (Colour on-line) Correlation between the astride character η_i of each mode (in abscissa), and its absorption efficiency computed as $Q_i^{-1} \times S_i^{\Omega_0}/S_i$, for three interfaces. Blue dots (respectively, green circles and red triangles) correspond to the zeroth (respectively, first and second) generation of the prefractal interface. One can first notice the direct correlation between the astride character of a mode and its absorption efficiency. Moreover, rougher interfaces exhibit a larger number of modes of high astride character, which corresponds to an increased absorption of the vibrations excited in the lossless region.

In order to efficiently contribute to the global damping of the cavity, a mode i must have both a small quality factor $Q_i = \mathrm{Re}(k_i)/\mathrm{Im}(k_i)$ and, for a source placed in the lossless region, a strong coupling to this source. So the absorption efficiency of a given mode ψ_i should be roughly proportional to the quantity $(S_i^{(\Omega_0)}/S_i)Q_i^{-1}$. When plotting this absorption efficiency against the astride character η_i for the modes of each interface (fig. 7), one can clearly see that both characteristics are closely correlated. Rougher interfaces exhibit simultaneously a larger number of modes of high astride character and large absorption efficiency. The average of the absorption efficiencies for the interfaces considered here (flat, rougher, and more rougher) are, respectively, proportional to 4, 6 and 7.5. The qualitative conclusion is that, due to the increase in the number of astride modes, geometrical irregularity favors dissipation. In other words: the more irregular, the better.

In summary, it was found in this study that the properties of 2D inhomogeneous resonators partially filled with an absorbing material strongly depend on the morphology of the interface separating the absorbing from the non-absorbing materials. For simple planar interface the modes split into two groups localized respectively in the absorbing and the non-absorbing regions. And, in first approximation, the complex spectrum is the union of the spectra associated with the separated absorbing and non-absorbing regions. The situation is very different with irregular interfaces. In the latter case, most of the modes live on both media, "astride" the irregular interface and the eigenvalue spectrum is not anymore the union of the separate spectra of the irregular regions. These facts are discussed here for a specific prefractal morphology but the same results can be obtained whatever the specific type of geometrical irregularity that is considered. Because they simultaneously display an important imaginary part to the eigenvalue and a larger amplitude in the non-absorbing region, the astride modes are thought to be important for the dissipation of wave energy emitted in the non-absorbing region. We believe that this constitutes the first simple rationale towards understanding the role of the absorbent geometry in anechoic chambers or wave-absorbing devices, would they be electromagnetic or acoustic [13–21]. The use (and theory) of reverberation chambers to measure the absorption of irregular panels should also be reconsidered in order to properly take into account the role of localization. But more generally, the same ideas should be useful in designing electromagnetic wave absorbers. In particular, they could explain how surface texturing at the scale of the wavelength may enhance photon energy conversion efficiency and decrease reflectance at silicon-air interface [22–24]. Astride localisation should also modify the surface emissivity and then Kirchoff's laws on porous surfaces. In the same manner, one may suggest that efficient break-waters should be more efficient if irregular at the scale of the wavelengths of sea-waves [25].

* * *

The authors wish to thank the French agencies ADEME and ANR for their financial support to this work (ADEME contract 0504C0045 and ANR project "Silent Wall" ANR-06-MAPR-0018).

REFERENCES

[1] Kerker M., *The Scattering of Light* (Academic Press, New York) 1969.

[2] Nieto-Vesperinas M., *Scattering and Diffraction in Physical Optics* (World Scientific, Singapore) 2006.

[3] Sakoda K., *Phys. Rev. B*, **72** (2005) 184201 and references therein.

[4] Daubert B. and Lapidus M. L., *Fractals*, **15** (3) (2007) 255 and references therein.

[5] Sapoval B., Gobron T. and Margolina A., *Phys. Rev. Lett.*, **67** (1991) 2974.

[6] Even C., Russ S., Repain V., Pieranski P. and Sapoval B., *Phys. Rev. Lett.*, **83** (1999) 726.

[7] Hébert B., Sapoval B. and Russ S., *J. Acoust. Soc. Am.*, **105** (1999) 1567.

[8] Félix S., Asch M., Filoche M. and Sapoval B., *J. Sound Vib.*, **299** (2007) 965.

[9] Asch M. and Lebeau G., *Exp. Math.*, **12** (2003) 227.

[10] Allard J. F., *Propagation of Sound in Porous Media - Modelling Sound Absorbing Materials* (Chapman & Hall, London) 1993. The results given in the paper have been obtained with the following parameters of the porous foam: porosity $\phi = 0.98$, tortuosity $\alpha_\infty = 1.2$, air flow resistivity $\sigma = 40000\,\mathrm{Nm^{-4}s}$, characteristic dimensions $\Lambda = 2\times10^{-4}$ m and $\Lambda' = 4\times10^{-4}$ m, and the cavity width a was taken equal to 0.2 m.

[11] Thouless D. J., *Phys. Rep.*, **67** (1980) 5.

[12] Russ S., Sapoval B. and Haeberlé O., *Phys. Rev. E*, **55** (1997) 1413.

[13] Hemming L. H., *Electromagnetic Anechoic Chambers: A Fundamental Design and Specification Guide* (Wiley-IEEE Press) 2002.

[14] Fractal Wall$^{\mathrm{TM}}$, product of Colas Inc., French patent No. 0203404; U.S. patent 10/508,119.

[15] Tsang L., Gu X. and Braunisch H., *IEEE Microw. Wirel. Compon. Lett.*, **16** (2006) 221.

[16] Chandler-Wilde S. N., Ross C. R. and Zhang B., *Proc. R. Soc. London, Ser. A*, **455** (1999) 3767.

[17] Jacobs E. L. and Lang R. H., *IEEE Trans. Antennas Propagat.*, **50** (2002) 1567.

[18] Saillard M., Popov E., Tsonev L., Scandella L. and Kruse N., *Appl. Opt.*, **34** (1995) 4883.

[19] Simon F., Rodriguez R. M. and Pfretzschner J., *J. Vib. Acoust.*, **124** (2002) 329.

[20] Sgard F. C., Olny X., Atalla N. and Castel F., *Appl. Acoust.*, **66** (2005) 625.

[21] Konz W., Hildenbrand J., Bauersfeld M., Hartwig S., Lambrecht A., Lehmann V. and Wollenstein J., *Smart Sensors, Actuators, and MEMS II, Proc. SPIE*, **5836** (2005) 540.

[22] Bright V. M., Kolesar E. S. and Sowders , *Opt. Eng., (Bellingham)*, **36** (1997) 1088.

[23] Raguin D. H. and Morris , *Appl. Opt.*, **32** (1993) 1154.

[24] Jansen H., Deboer M., Burger J., Legtenberg R. and Elwenspock M., *J. Micromech. Eng.*, **5** (1995) 475.

[25] US Army Coastal Engineering Research, *Shore Protection Manual*, Vol. **2** (Department of the Army Waterways Experimental Station, Vicksburg, MS) 1984.